

# The Crystal and Solution Structures of the Major Products of the Reaction of Vanadate with Adenosine

Sarah J. Angus-Dunne, Raymond J. Batchelor, Alan S. Tracey,\* and Frederick W. B. Einstein

Contribution from the Department of Chemistry, Simon Fraser University, Burnaby, B.C. V5A 1S6, Canada

Received December 1, 1994<sup>⊗</sup>

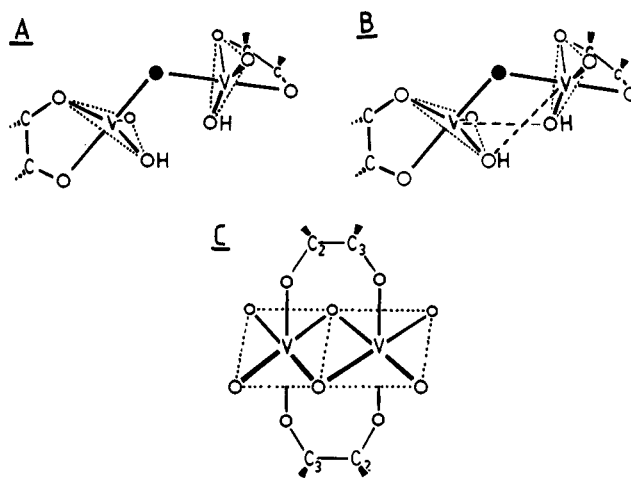
**Abstract:** A crystalline product of the reaction of adenosine with vanadate has been obtained from aqueous solution. Its structure has been determined from X-ray diffraction studies and this structure related to the products of equilibration in aqueous solution. The crystalline product was found to contain two vanadium nuclei and two adenosine moieties in a dimeric structure. Each vanadium was coordinated in an irregular pentacoordinate arrangement. <sup>1</sup>H and <sup>51</sup>V timecourse NMR studies at reduced temperature in acetone/water solvent provided strong evidence that the crystal structure was maintained in solution and that related structures were the source of the other major products found in equilibrated solutions. Crystal structure of [NEt<sub>4</sub>]<sub>2</sub>[VO<sub>2</sub>Ad]<sub>2</sub> · 4.74H<sub>2</sub>O: monoclinic, space group P2<sub>1</sub>; Z = 2; a = 13.676(2) Å; b = 11.625(2) Å; c = 15.306(2) Å; β = 95.525(9)°; V = 2422.0 Å<sup>3</sup>; T = 200 K; R<sub>F</sub> = 0.029 for 4400 data (I<sub>o</sub> ≥ 2.5σ(I<sub>o</sub>)) and 652 variables.

## Introduction

The interest in the reactions between vanadate and nucleosides first arose when it was shown that a vanadate/uridine complex was a potent inhibitor of bovine ribonuclease A.<sup>1</sup> This early work gave rise to a representation of the adenosine/vanadate/ribonuclease A complex that was exceptionally accurate as later found from crystal structure studies.<sup>2</sup>

Although it was initially assumed that the vanadate/uridine complex contained a single vanadate and a single uridine, <sup>51</sup>V NMR studies of vanadate in the presence of various diols,<sup>3,4</sup> monosaccharides,<sup>4,5</sup> and nucleosides<sup>5-9</sup> revealed a ubiquitous 2:2 stoichiometry. A trigonal-bipyramidal structure was predicted for the coordination about each vanadium of the complex, after the fashion depicted in Chart 1, structure A.<sup>3</sup> It was later recognized that the vanadiums were complexed in a multicyclic ring system. The trigonal-bipyramidal structure could possibly be distorted toward octahedral coordination by participation of the equatorial OH residues of one vanadium of the dimeric complex in bonding with the second vanadium. Structure B (Chart 1) and variants thereof were then proposed<sup>7</sup> in part to account for the chemical exchange pattern and the number of isomeric products observed. Other workers disputed this coordination and, on the basis of optical magnetic resonance studies, suggested an octahedral coordination with bridging between the vanadium nuclei, as shown in Chart 1, structure C.<sup>10,11</sup> This structure cannot account for the observed major products without invoking coordination changes. X-ray struc-

Chart 1



tures of related dinuclear complexes of chlorovanadate with pinacol<sup>12</sup> and of vanadate with 2-hydroxy-2-ethylbutanoate<sup>13</sup> did not show any of the above structures, but instead a core containing a VOVO four-membered ring, with each vanadium in a distorted trigonal-bipyramidal arrangement, was found. This structure, however, did not carry over to a dimeric chlorovanadate complex with ethylene glycol where a macrocyclic arrangement of tetrahedral vanadiums was observed.<sup>14</sup> It is evident from this that considerable ambiguity exists and the structures of nucleoside complexes with vanadate are not known with any degree of certainty.

Recently, we have been able to obtain a crystalline vanadate/adenosine complex suitable for X-ray structure analysis. By using a mixed solvent system at reduced temperature, it was possible to slow the rate of equilibration of the dissolved crystalline material so that <sup>51</sup>V and <sup>1</sup>H NMR spectroscopy could

<sup>⊗</sup> Abstract published in *Advance ACS Abstracts*, May 1, 1995.

(1) Lindquist, R. N.; Lynn, J. L., Jr.; Lienhard, G. E. *J. Am. Chem. Soc.* **1973**, *95*, 8762-8768.

(2) Borah, B.; Chen, C.-W.; Egan, W.; Miller, M.; Wlodawer, A.; Cohen, J. S. *Biochemistry* **1985**, *24*, 2058-2067.

(3) Gresser, M. J.; Tracey, A. S. *J. Am. Chem. Soc.* **1986**, *108*, 1935-1939.

(4) Tracey, A. S.; Gresser, M. J. *Inorg. Chem.* **1988**, *27*, 2695-2702.

(5) Geraldès, F. G. C.; Castro, M. M. C. A. *J. Inorg. Biochem.* **1989**, *35*, 79-93.

(6) Zhang, X.; Tracey, A. S. *Acta Chem. Scand.* **1992**, *46*, 1170-1176.

(7) Tracey, A. S.; Leon-Lai, C. H. *Inorg. Chem.* **1991**, *30*, 3200-3204.

(8) Tracey, A. S.; Jaswal, J. S.; Gresser, M. J.; Rehder, D. *Inorg. Chem.* **1990**, *29*, 4283-4288.

(9) Richter, J.; Rehder, D. Z. *Naturforsch.* **1991**, *46b*, 1613-1620.

(10) Crans, D. C.; Harnung, S. E.; Larsen, E.; Shin, P. K.; Theisen, L. A.; Trabjerg, I. *Acta Chem. Scand.* **1991**, *45*, 456-462.

(11) Harnung, S. E.; Larsen, E.; Pedersen, E. J. *Acta Chem. Scand.* **1993**, *47*, 674-682.

(12) Crans, D. C.; Felty, R. A.; Miller, M. M. *J. Am. Chem. Soc.* **1991**, *113*, 265-269.

(13) Hambley, T. W.; Judd, R. J.; Lay, P. A. *Inorg. Chem.* **1992**, *31*, 343-345.

(14) Crans, D. C.; Felty, R. A.; Anderson, O. P.; Miller, M. M. *Inorg. Chem.* **1993**, *32*, 247-248.

be used to relate the structure of the crystalline material to that in aqueous solution.

## Experimental Section

**Materials.** Vanadium pentoxide (Fischer Scientific, 99.9%), adenosine (Sigma Chemical Co.), tetraethylammonium hydroxide (20% aqueous solution, Sigma Chemical Co.), hydrochloric acid (1 N aqueous solution, Fischer Scientific), and acetone-*d*<sub>6</sub> (ISOTECH, Inc.) were used as supplied.

Spectrograde acetone (Caledon, 99.5%) was purified by the addition of 2 g of AgNO<sub>3</sub> in 10 mL H<sub>2</sub>O to 500 mL of acetone followed by 5 mL of 1 M NaOH.<sup>15</sup> The mixture was shaken for 10 min, filtered, then dried over CaSO<sub>4</sub> (drierite) before being distilled from fresh CaSO<sub>4</sub>. The distilled product was redistilled twice more from fresh CaSO<sub>4</sub>. No unexpected <sup>51</sup>V NMR signals were observed when a 1 mmol/L (Et<sub>4</sub>N)<sub>2</sub>HVO<sub>4</sub> solution was prepared in the purified acetone (1% H<sub>2</sub>O).

**(Et<sub>4</sub>N)<sub>2</sub>HVO<sub>4</sub>:** The stock vanadate solution used in these studies, 100 mM (Et<sub>4</sub>N)<sub>2</sub>HVO<sub>4</sub>, was prepared by the dissolution of 0.455 g (2.5 mmol) of V<sub>2</sub>O<sub>5</sub> in 7.40 g of 20% aqueous Et<sub>4</sub>NOH followed by dilution to 50 mL with distilled H<sub>2</sub>O.

**[NEt<sub>4</sub>]<sub>2</sub>{VO<sub>2</sub>Ad<sub>2</sub>]<sub>2</sub>:** Adenosine (0.267 g, 1 mmol) was added to a stirred aqueous solution (10 mL) of 100 mmol/L (Et<sub>4</sub>N)<sub>2</sub>HVO<sub>4</sub> at pH 10. The pH of the solution was adjusted to pH 6.5 using 0.1 M HCl and the solution was warmed to 50 °C for 30 min. The container was partially covered with parafilm to allow slow evaporation and placed in a refrigerator at 3 °C. After 12 weeks small crystals had formed. In order to encourage crystal growth, the crystalline product was partially redissolved by small additions of H<sub>2</sub>O (0.1 mL) several times over a period of 4 weeks. A crystal was selected for X-ray studies and the remaining pale yellow crystals were recovered by filtration (yield 20%, 0.208 g). This material was recrystallized from aqueous solution. Anal. Expected for (Et<sub>4</sub>N)<sub>2</sub>(VO<sub>2</sub>C<sub>10</sub>N<sub>5</sub>O<sub>2</sub>H<sub>11</sub>)<sub>2</sub> · 5H<sub>2</sub>O (1046.9 g/mol): C, 41.3; H, 6.93; N, 16.06. Found: C, 41.05; H, 7.05; N, 15.90. IR (selected stretches) 1482 s, 1391 m, 1335 m, 1309 m, 1191 m, 1119 s, 1081 s, 919 s, 911 s, 869 m, 753 m, 647 m. For an IR spectrum see the supplementary material.

**X-ray Analysis.** A plate-shaped crystal was removed from the mother-liquor and cleaved to yield a single-crystal fragment of suitable size. With a trace of apiezon grease as adhesive, the fragment was gently wedged inside a glass capillary tube, which was then sealed. Data (*h, k, l*) were recorded at 200 K with an Enraf Nonius CAD4F diffractometer equipped with an in-house modified low-temperature attachment and using graphite monochromatized Mo K $\alpha$  radiation. Two standard reflections were measured every hour of exposure time and were found to fluctuate in intensity by  $\pm 2\%$  during the course of the measurements. The data were corrected for absorption by the Gaussian integration method. Data reduction included corrections for intensity scale variation and for Lorentz and polarization effects.

The structure was solved by direct methods and elaborated by Fourier and least-squares techniques. Sites for all non-hydrogen atoms of one formula unit of the complex salt plus five water molecules of crystallization in the asymmetric unit were located. One water site was found to be only partially occupied and an occupancy parameter for this oxygen atom was included in the refinement (final refined occupancy = 0.743(6)). Anisotropic thermal parameters for all non-hydrogen atoms were refined subject to null motion restraints for bonded pairs. These restraints were later released in the final cycles of full-matrix least-squares refinement.

Peaks attributable to most of the hydrogen atoms were located in an electron density difference map. Nonetheless, hydrogen atoms were included in calculated positions bonded to appropriate C and N atoms and were made to ride on them during structure refinement. Hydrogen atoms of the OH groups and the H<sub>2</sub>O molecules were placed at appropriate peak positions from the difference map and their positional coordinates were refined subject to reasonable, soft distance restraints. These restraints were retained in the final cycles of refinement. Initial isotropic temperature factors for the hydrogen atoms were assigned according to the equivalent isotropic thermal motion of their respective C, N, or O atoms. Ultimately, an isotropic thermal motion parameter

was refined for each of eleven different groups of chemically similar hydrogen atoms and the shifts were applied to the individual values.

The four fully occupied water sites were found to be hydrogen-bonded to the discrete complex anions. Two of these water molecules also form a H-bonded pair. The other two were found to be H-bonded to the partially occupied water site—which itself is not H-bonded to the anions. The most significant difference map feature at this stage indicated that the position of one of the water oxygen atoms, which was hydrogen-bonded to the fractionally occupied water molecule, shifts somewhat into the void formed when the latter is not present. The positions of two sites for the former oxygen atom were refined with fractional occupancy parameters constrained to correlate with that of the partially “lost” molecule and to total 1 for the site.

The difference map also indicated some disorder of one of the NEt<sub>4</sub><sup>+</sup> ions which show, in either case, approximate  $\bar{4}m2$  (*D*<sub>2d</sub>) point symmetry. This disorder consists of a small percentage contribution from an approximately inverted arrangement for the ion accompanied by a slight tilting such that three of the methyl carbon atom positions and the nitrogen atom position approximately overlap with (but the fourth methyl-carbon atom site diverges slightly from) those of the major orientation. Rigid-group positional parameters for central N(CH<sub>2</sub>)<sub>4</sub> fragments for the two orientations were refined with fractional occupancies constrained to total 1 (the final occupancy for the major orientation was 0.909(5)). Independent positional parameters for five methyl-carbon atom sites (three at unit occupancy and two constrained to have the occupancies of their respective N(CH<sub>2</sub>)<sub>4</sub> fragments) were refined subject to reasonable C(H<sub>3</sub>)–C(H<sub>2</sub>) and C(H<sub>3</sub>)–N distance restraints. Hydrogen atoms of appropriate occupancies and isotropic temperature factors were included in calculated positions and those of the methyl groups were made to ride on their respective carbon atoms. Anisotropic thermal parameters were retained (and refined) for the carbon atom sites corresponding to the major orientation of the ion. The carbon atom sites belonging exclusively to the minor orientation were initially assigned isotropic thermal parameters estimated from the equivalent isotropic thermal parameters for the atoms of that chemical type and a single parameter was refined for their thermal motion and its shifts applied to the individual values. A single isotropic thermal parameter was refined for the nitrogen atom. Hydrogen atom isotropic temperature factors were treated as discussed above.

A weighting scheme based on counting statistics was applied such that  $\langle w(|F_o| - |F_c|)^2 \rangle$  was near constant as a function of both  $|F_o|$  and  $\sin\theta/\lambda$ . Final full-matrix least-squares refinement of 652 parameters for 4400 data ( $I_o \geq 2.5\sigma(I_o)$ ) and 39 restraints converged at  $R = 0.029$ . The final maximum  $|\text{shift}/\text{error}|$  was 0.01. Crystallographic details are summarized in Table 1. Final fractional atomic coordinates for all atoms are listed in the supplementary material. The computer programs used were from the NRCVAX Crystal Structure System<sup>16</sup> and from CRYSTALS<sup>17</sup> which was used for the structure refinement. Complex scattering factors for neutral atoms<sup>18</sup> were used in the calculation of structure factors. Computations were carried out on MicroVAX-II and 80486 computers.

The polarity of the structure as reported here is consistent with that expected for the naturally occurring nucleoside. Nonetheless, this was corroborated by including the Flack Enantiopole parameter<sup>19</sup> in one further cycle of full-matrix least-squares refinement of the structure. The parameter did not shift significantly from zero ( $-0.06(4)$ ).

**NMR Studies. Vanadium spectra:** All NMR spectra were obtained on a Bruker AMX-400 NMR spectrometer operating at 258 K. <sup>51</sup>V NMR spectra were obtained using an 80 kHz spectral width, a 0.04 s acquisition time, a 60° pulse width, and 3000 scans. Vanadium chemical shifts are given relative to an external reference VOCl<sub>3</sub> via a calibrated intermediate reference of concentrated trisodium vanadate in water. All spectra were processed using a 40 Hz line-broadening factor and a 32 K transform size.

(16) Gabe, E. J.; LePage, Y.; Charland, J.-P.; Lee, F. L.; White, P. S. J. *Appl. Crystallogr.* **1989**, *22*, 384.

(17) Watkin, D. J.; Carruthers, J. R.; Betteridge, P. W. *CRYSTALS*; Chemical Crystallography Laboratory, Oxford University: Oxford, England, 1984.

(18) *International Tables for X-ray Crystallography*; Kynoch Press: Birmingham, 1975; Vol. IV, pp 99.

(19) Flack, H. *Acta Crystallogr.* **1983**, *A39*, 876–881.

(15) Perrin, D. D.; Armarego, W. L. F. *Purification of Laboratory Chemicals*, 3rd ed.; Pergamon Press: Oxford, New York, 1988.

**Table 1.** Crystallographic Data for the Structure Determination of  $[\text{NEt}_4]_2[\{\text{VO}_2\text{Ad}\}_2] \cdot 4.743\text{H}_2\text{O}$  at 200 K

formula	$\text{V}_2\text{O}_{16.743}\text{N}_{12}\text{C}_{36}\text{H}_{71.486}$
fw	1042.29
crystal system	monoclinic
space group	$P2_1$
$a$ (Å) <sup>a</sup>	13.676(2)
$b$ (Å)	11.625(2)
$c$ (Å)	15.306(2)
$\beta$ (deg)	95.525(9)
$V$ (Å <sup>3</sup> )	2422.0
$Z$	2
temp (K)	200
$\rho_c$ (g cm <sup>-3</sup> )	1.429
$\lambda$ (Mo K $\alpha_1$ ) (Å)	0.70930
$\mu$ (Mo K $\alpha$ ) (cm <sup>-1</sup> )	4.5
min - max $2\theta$ (deg)	4-52
transmission <sup>b</sup>	0.849-0.880
cryst dimens (mm)	0.36 × 0.37 × 0.38
GoF <sup>c</sup>	1.52
$R_F$ <sup>d</sup>	0.029
$R_{wF}$ <sup>e</sup>	0.034

<sup>a</sup> Cell dimensions were determined from 25 reflections ( $34.5^\circ \leq 2\theta \leq 43.0^\circ$ ). <sup>b</sup> The data were corrected for the effects of absorption by the Gaussian integration method. <sup>c</sup> GoF =  $[\sum(w(F_o - F_c)^2)/(\text{degrees of freedom})]^{1/2}$ . <sup>d</sup>  $R_F = \sum(|F_o| - |F_c|)/\sum|F_o|$ , for 4400 data ( $I_o \geq 2.5\sigma(I_o)$ ). <sup>e</sup>  $R_{wF} = [\sum(w(|F_o| - |F_c|)^2)/\sum(wF_o^2)]^{1/2}$  for 4400 data ( $I_o \geq 2.5\sigma(I_o)$ );  $w = [\sigma(F_o)^2 + 0.0002F_o^2]^{-1}$ .

Approximately 2 mg of the powdered crystalline product were placed in a 10 mm NMR tube and then cooled to 253 K. A solution consisting of 1 mL of purified acetone and 1 mL of distilled water, also at 253 K, was added to the NMR tube and the tube was stoppered, shaken, and transferred immediately to the NMR probe. Previous studies showed that, under such conditions, the powdered crystalline product dissolved within a few seconds.

**Proton spectra:** A spectral window of 5000 Hz, a line-broadening factor of 1 Hz, and a 60° pulse width with a 1 s relaxation delay were used for all spectra. For the short time spectra of the kinetic runs eight spectra were acquired, but this was increased to 64 spectra for the longer times.

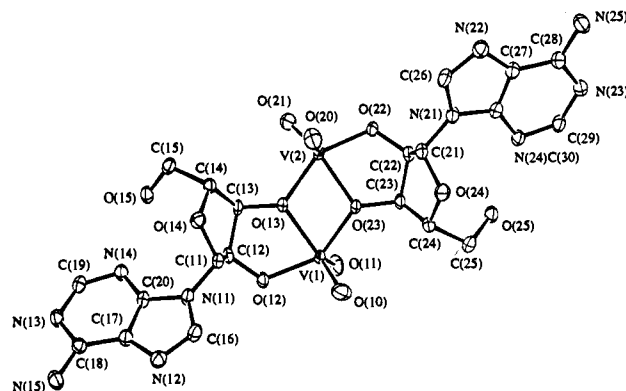
Approximately 0.5 mg of the powdered crystalline material was treated as described above for the vanadium spectra, with the exception that a solution consisting of 0.3 mL of deuterated acetone and 0.3 mL of deuterated water was used in a 5 mm NMR tube.

Final vanadium and proton kinetic runs were monitored for a total of 140 min.

## Results

**X-ray Structure Analysis.** The crystallization from concentrated aqueous solution of an adenosine complex provided a near-colorless plate-like crystalline material suitable for X-ray structure analysis. The molecular structure of the complex anion is shown in Figure 1. Selected intramolecular distances and angles are given in Table 2. The anion diverges from an approximate local 2-fold rotational symmetry most significantly in the arrangements of ligating atoms about the two vanadium atoms. For example, the only pair of pseudo-2-fold-related bond lengths which differ significantly from one another are V(1)-O(12) (1.939(2) Å) and V(2)-O(22) (1.916(2) Å). Interestingly, the largest deviation (45.3°) between pseudo-2-fold-related bond torsion angles is between O(23)-V(1)-O(12)-C(12) -9.9-(1)° and O(13)-V(2)-O(22)-C(22) -55.2(2)°, where the more nearly eclipsed arrangement corresponds to the longer central V-O bond length. The largest pseudo-2-fold-related bond angle deviations are between O(10)-V(1)-O(13) 128.0(1)° and O(20)-V(2)-O(23) 109.7(1)° and between O(11)-V(1)-O(13) 122.4(1)° and O(21)-V(2)-O(23) 141.9(1)°.

These differences presumably arise because of the nature of the crystal packing and the different arrangements for hydrogen bonding between water molecules and the oxygen atoms

**Figure 1.** The molecular structure of  $[\{\text{VO}_2\text{Ad}\}_2]^{2-}$  at 200 K viewed along the  $b$ -axis. 50% probability thermal ellipsoids are shown for all non-hydrogen atoms. Hydrogen atoms have been omitted.**Table 2.** Selected Intramolecular Distances (Å) and Angles (deg) for  $[\text{NEt}_4]_2[\{\text{VO}_2\text{Ad}\}_2] \cdot 4.743\text{H}_2\text{O}$  at 200 K

V(1)-O(10)	1.625(2)	V(2)-O(20)	1.633(3)
V(1)-O(11)	1.626(3)	V(2)-O(21)	1.630(2)
V(1)-O(12)	1.939(2)	V(2)-O(22)	1.916(2)
V(1)-O(13)	2.036(2)	V(2)-O(23)	2.042(2)
V(1)-O(23)	1.983(2)	V(2)-O(13)	1.976(2)
O(12)-C(12)	1.396(3)	O(22)-C(22)	1.410(3)
O(13)-C(13)	1.421(3)	O(23)-C(23)	1.422(3)
O(14)-C(11)	1.412(3)	O(24)-C(21)	1.410(3)
O(14)-C(14)	1.459(4)	O(24)-C(24)	1.455(4)
N(11)-C(11)	1.455(3)	N(21)-C(21)	1.452(4)
C(11)-C(12)	1.536(4)	C(21)-C(22)	1.535(5)
C(12)-C(13)	1.526(4)	C(22)-C(23)	1.526(4)
C(13)-C(14)	1.518(4)	C(23)-C(24)	1.518(4)
C(14)-C(15)	1.510(4)	C(24)-C(25)	1.510(4)
O(10)-V(1)-O(11)	109.3(1)	O(21)-V(2)-O(20)	107.9(1)
O(10)-V(1)-O(12)	101.2(1)	O(20)-V(2)-O(22)	104.9(1)
O(11)-V(1)-O(12)	99.0(1)	O(21)-V(2)-O(22)	98.3(1)
O(10)-V(1)-O(13)	128.0(1)	O(20)-V(2)-O(23)	109.7(1)
O(11)-V(1)-O(13)	122.4(1)	O(21)-V(2)-O(23)	141.9(1)
O(12)-V(1)-O(13)	78.18(8)	O(22)-V(2)-O(23)	78.15(8)
O(10)-V(1)-O(23)	97.9(1)	O(13)-V(2)-O(20)	102.5(1)
O(11)-V(1)-O(23)	99.3(1)	O(13)-V(2)-O(21)	96.6(1)
O(12)-V(1)-O(23)	147.36(8)	O(13)-V(2)-O(22)	142.82(9)
O(13)-V(1)-O(23)	69.20(8)	O(13)-V(2)-O(23)	69.21(8)
V(1)-O(12)-C(12)	117.5(2)	V(2)-O(22)-C(22)	115.1(2)
V(1)-O(13)-V(2)	110.68(9)	V(1)-O(23)-V(2)	110.18(9)
V(1)-O(13)-C(13)	118.1(2)	V(2)-O(23)-C(23)	118.8(2)
V(2)-O(13)-C(13)	128.7(2)	V(1)-O(23)-C(23)	128.3(2)
C(11)-O(14)-C(14)	109.6(2)	C(21)-O(24)-C(24)	109.8(2)
O(14)-C(11)-C(12)	107.1(2)	O(24)-C(21)-C(22)	106.8(2)
O(12)-C(12)-C(11)	113.7(3)	O(22)-C(22)-C(21)	112.5(3)
O(12)-C(12)-C(13)	111.4(2)	O(22)-C(22)-C(23)	111.3(2)
C(11)-C(12)-C(13)	101.0(2)	C(21)-C(22)-C(23)	102.1(2)
O(13)-C(13)-C(12)	103.7(2)	O(23)-C(23)-C(22)	104.5(2)
O(13)-C(13)-C(14)	111.8(2)	O(23)-C(23)-C(24)	112.6(2)
C(12)-C(13)-C(14)	104.6(2)	C(22)-C(23)-C(24)	104.4(2)
O(14)-C(14)-C(13)	106.3(2)	O(24)-C(24)-C(23)	107.1(2)
C(13)-C(14)-C(15)	113.8(3)	C(23)-C(24)-C(25)	114.1(3)

attached to vanadium. In the absence of such interactions, the complex would have 2-fold symmetry.

**Nuclear Magnetic Resonance Studies.** (a) <sup>51</sup>V NMR spectroscopy: A <sup>51</sup>V NMR study (at 3 °C) of a solution prepared from material taken from the crystalline mass from which the crystal used for the X-ray work was obtained showed the possible presence of more than one product. Product signals were observed at -517 ppm (a very broad signal) and at -552 and -569 ppm, with the major signal occurring at -517 ppm. After a few minutes of equilibration, a more typical set of vanadium signals, for which the -552 and -569 ppm signals were absent, was obtained. In addition, the broad signal

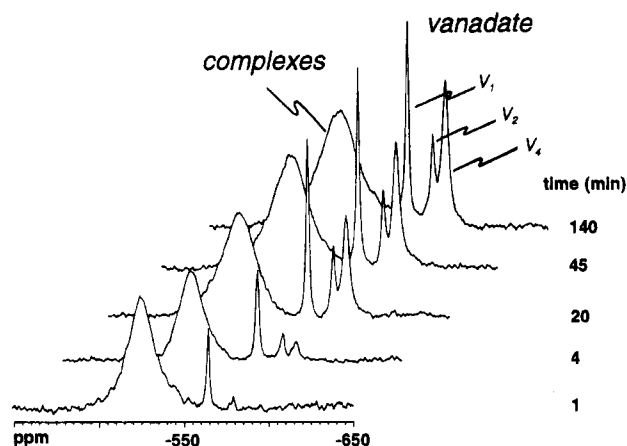


**Figure 2.** Vanadium-51 NMR timecourse study of the equilibration of the  $[\{VO_2Ad\}_2]^{2-}$  complex at  $-15\text{ }^\circ\text{C}$  in 50% acetone/water. The solution contained approximately 1 mg/mL of the complex. No pH adjustment was carried out,  $\text{pH} \approx 7$ .

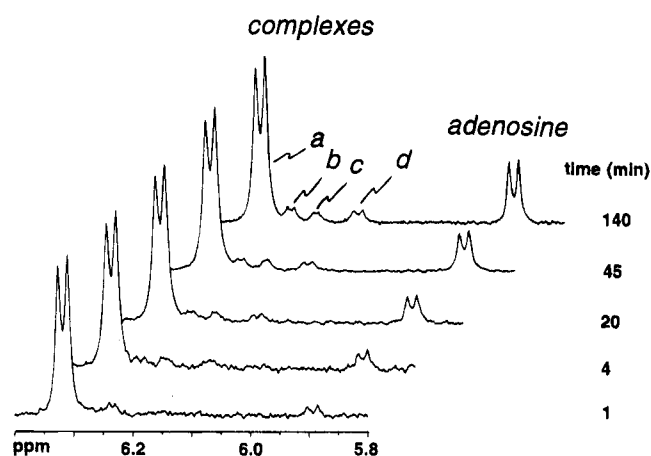


**Figure 3.** Proton NMR timecourse study of the equilibration of the  $[\{VO_2Ad\}_2]$  dianion at  $-15\text{ }^\circ\text{C}$  in 50% acetone- $d_6/D_2O$ . Only the signals of the anomeric proton of the various ribose rings are shown. The solution contained approximately 0.8 mg/mL of the complex. No adjustment of the pH was carried out,  $\text{pH} \approx 7$ .

centered near  $-517\text{ ppm}$  sharpened into a signal at  $-522\text{ ppm}$ . Signals for monomeric vanadate and its oligomers were also obtained. In view of the possibility of multiple products, the initially obtained crystalline material was recrystallized. The resultant material provided a single product with a signal at  $-522\text{ ppm}$ . An X-ray measurement of unit cell dimensions for a crystal selected from the recrystallized product revealed a unit cell similar to that of the original crystal but with a slightly reduced volume (by  $20\text{ \AA}^3$ ). This small volume change is ascribed to loss of the loosely bound water found in partial occupancy in the original crystal rather than to a change in structure of the anion (see Experimental Section).

Initial studies showed that in water, at  $3\text{ }^\circ\text{C}$ , the rate of equilibration of the crystalline material was too fast to obtain detailed information about the equilibration process. However, it was found that a 1:1 acetone/water solution did not seriously decrease the rate of dissolution of the crystals at  $-20\text{ }^\circ\text{C}$ . The powdered crystalline product was dissolved at  $-20\text{ }^\circ\text{C}$  in an NMR tube and placed immediately in the NMR probe, regulated at  $-15\text{ }^\circ\text{C}$ . Figure 2 shows a sequence of vanadium spectra following dissolution of the product. The process of equilibration leads to the formation of uncomplexed vanadate and the indicated oligomers. There was no measurable change in the position of the  $-522\text{ ppm}$  signal with time. This strongly

suggested that there was no change in coordination about the vanadium after dissolution.

**(b)  $^1\text{H}$  NMR spectroscopy:** Detailed studies have shown that at low ionic strength, four sets of product signals are readily observable in the proton spectrum.<sup>6</sup> Figure 3 shows the sequential changes in the anomeric region of the spectrum of adenosine after dissolution occurs. The signal at  $6.32\text{ ppm}$  (signal *a*) apparently arises from material corresponding to the crystalline product while the signal at  $5.89\text{ ppm}$  is known to arise from the free ligand.<sup>6,8</sup> One additional product signal is clearly visible (signal *c*,  $6.24\text{ ppm}$ ) at a short time after dissolution. Two additional signals,  $6.27\text{ ppm}$  (signal *b*) and  $6.16\text{ ppm}$  (signal *d*), arise more slowly.

Complete  $^{13}\text{C}$  and  $^1\text{H}$  chemical and coordination shifts have been reported for the major products of the reaction of vanadate with adenosine and with inosine.<sup>6,7</sup> The proton-proton coupling constants were also reported and the conformation of the ribose ring in the major products deduced. The present NMR studies were not as detailed as those of the previous work.<sup>6,7</sup> However, no discrepancies between this and the earlier work were noted.

The NMR results obtained here and the chemical exchange studies previously reported<sup>7</sup> can be amalgamated into a coherent picture using the structure of the crystalline material as a basis.

## Discussion

It is becoming more and more clear that the cyclic VOVO fragment of the adenosine complex studied here represents a characteristic property of vanadate binuclear complexes. A similar arrangement is found in polymeric "metavanadate" as well as in a number of other complexes,<sup>20</sup> including crystalline trimethoxyvanadate<sup>21</sup> and an ethylenediamine Schiff base derived dimer.<sup>22</sup> A similar structural motif is found in a complex of vanadate with an  $\alpha$ -hydroxy acid<sup>13</sup> and in a pinacol/chlorovanadate complex.<sup>12</sup>

In the adenosine derivative described here, the  $(VO)_2$  four-membered ring is close to a parallelogram with the two pairs of sides being  $2.036(2)\text{ \AA}$  ( $V(1)-O(13)$ ) and  $2.042(2)\text{ \AA}$  ( $V(2)-O(23)$ ), respectively, in one dimension and  $1.983(2)\text{ \AA}$  ( $V(1)-O(23)$ ) and  $1.976(2)\text{ \AA}$  ( $V(2)-O(13)$ ) in the other. The internal angles are close to  $110.5^\circ$  (at O) and  $69.2^\circ$  (at V) for the two vertices (see Table 2). The longer sides each form a five-membered ring with the ribose of the adenosine ligand and are presumably elongated because of strain caused by the adjacent five-membered ribose ring with which it shares a common edge. A similar distortion is not observed in the structure of the related compound  $[\text{NH}_4]_2[\{VO_2(\text{OC}(\text{CH}_2\text{CH}_3)_2\text{COO})\}_2]$  where all sides are of comparable length,  $1.973(2)$  and  $1.984(2)\text{ \AA}$  respectively for the two distinct sides. The internal angles in this case are  $104.0(2)^\circ$  and  $71.9(1)^\circ$ .<sup>13</sup> (Note that these two angles are reversed from the assignment given in ref 13.) This near equality of side lengths is also found in a chlorovanadate complex with pinacol where the two types of V-O bonds have lengths of  $1.967(1)$  and  $1.964(1)\text{ \AA}$  with internal angles of  $108.6(1)^\circ$  and  $71.4(1)^\circ$ .<sup>12</sup> In contrast to this, in a tris(cyclopentanato)-oxovanadium(V) dimeric complex the two lengths are very different, the V-O bond being  $1.835(4)\text{ \AA}$  within the monomeric unit of the dimer and  $2.296(3)\text{ \AA}$  between the two units. Despite the large differences in distances, the internal angles of the parallelogram were not much different from those of the other derivatives being  $108.2(2)^\circ$  and  $71.9(2)^\circ$ .<sup>23</sup>

(20) Holloway, C. E.; Melnik, M. *Rev. Inorg. Chem.* **1985**, *7*, 75-159.

(21) Priebisch, W.; Rehder, D. *Inorg. Chem.* **1990**, *29*, 3013-3019.

(22) Colpas, G. J.; Hamstra, B. J.; Kampf, J. W.; Pecoraro, V. L. *Inorg. Chem.* **1994**, *33*, 4669-4675.

(23) Hillerns, F.; Olbrich, F.; Behrens, U.; Rehder, D. *Angew. Chem., Int. Ed. Engl.* **1992**, *31*, 447-448.

The structures about the two vanadium centers of the dimer differ to an extent from each other. The angles O(21)V(2)O(23) = 141.9(1)° and O(13)V(2)O(22) = 142.8(1)° reveal close to a square pyramidal coordination about V(2). For the case of V(1), the coordination is much more irregular. The angles corresponding to the above are O(10)V(1)O(13) = 128.0(1)° and O(12)V(1)O(23) = 147.4(1)°. Distances from VO oxygen atoms to the water oxygen sites are O(22)–O = 2.711(4) Å, O(20)–O = 2.740(4) Å, O(12)–O = 2.791(4) Å, O(10)–O = 2.915(4) Å. These distances correspond only to relatively weak hydrogen-bonding interactions. There are no secondary interactions involving either vanadium atom; the shortest distance between a water oxygen and a vanadium atom is 3.97 Å. A table of distances and angles for all atoms involved in hydrogen-bonding interactions is provided in the supplementary material.

The weak hydrogen-bonding interactions between the anion and the water in the crystal suggests that there will be only small modifications in the structure when it is dissolved into aqueous medium. Dissolution of the adenosine complex at –15 °C into 50% acetone/water initially gives rise to a single signal, both in the vanadium spectrum (Figure 2) and in the proton spectrum of the anomeric proton of the ribose ring (Figure 3). The chemical shifts corresponding to the initial signals do not vary with time although the process of equilibration leads to the generation of additional products. These products are observable as well-resolved signals in the proton spectrum but only as asymmetry in the vanadium signal. This small effect on the vanadium spectrum suggests that the products of equilibration have the same coordination about vanadium as the original material.

Previous proton NMR studies of the complexes, in aqueous solution, have shown that the ribose ring of the free ligand and of the major product (**a** of Figure 3) has a predominant conformation encompassed within the range of  ${}^2E-{}^2T_1-E_1$  conformations.<sup>7</sup> The rings in the crystalline material show distorted  ${}^2T_1$  twist conformations with a predominance of  ${}^2E$  envelope character. The proton solution studies, therefore, are consistent with no major structural difference between the crystalline material and product **a** of Figure 3.

It has been shown from chemical exchange studies that the equilibration between the species giving rise to the signals **a** and **c** and also between **b** and **d** occurs much more rapidly than that between the two sets of products or between either set and the free ligand.<sup>7</sup> The present result is in full accord with this, as product **c** is formed quite quickly from **a** while the buildup of the free ligand and of the **b** and **d** product occurs much more slowly.

A clue to the equilibration process that explains all the observations is found in the structure of a vanadium(V) chloride complex with ethylene glycol [(VOCl(OCH<sub>2</sub>CH<sub>2</sub>O))<sub>2</sub>].<sup>14</sup> In this material, the glycol bridges between two tetrahedrally coordinated vanadiums to form a 10-membered macrocyclic structure. It is evident from Figure 1 that a similar macrocycle can be formed with the adenosine complex studied here if the V(1)–O(13) and V(2)–O(23) bonds are simultaneously broken. These represent the two long V–O bonds in the crystal structure and they presumably will be more easily opened than the alternative pair.

The initial product, **a** (signal **a** of Figure 3), can be regenerated by a recyclicalization. However, a shift in relative positions within the intermediate macrocycle will allow cyclization from V(1) to O(22) and V(2) to O(12) to occur. This second product, **c**, will be a structural isomer of **a** and correspond to signal **c** of Figure 3. Both **a** and **c** have a 2-fold symmetry axis so each gives rise to only one NMR signal for the two adenosine rings.

On the 1-s time scale, at 275 K, no exchange from signals **a** or **c** to **b** or **d** was observed nor was any exchange to the free ligand found.<sup>7</sup> Simultaneous breaking of the V(1)–O(13) and V(2)–O(23) bonds generates the macrocycle discussed above. It is reasonable to speculate that, instead of these two bonds breaking, the V(1)–O(23) and V(2)–O(13) bonds could break to give the monomeric precursor to the crystalline product. The buildup of signals, **b** and **d** of Figure 3, occurs fairly quickly relative to that of the free ligand. The results suggest that the monomer redimerizes faster than it dissociates to release free ligand. If, after dimerization occurs, one monomeric unit has rotated 180° relative to the first, a third isomeric product will be formed. The two adenosine residues in this material are chemically distinct so that this product will give rise to two adenosine signals of equal intensity. There are no other possible isomeric products for this coordination geometry and the proton NMR signals occur in pairs, **a,c** for the two symmetrical products, **a** and **c**, and **b,d** for the one asymmetrical product, **b**. The two adenosine moieties in **b** are rapidly interchanged by the same mechanism that interconverts **a** and **c** and this explains why the exchange rates for the two systems are similar.<sup>7</sup>

Previous work has shown that at high ionic strength (1 M KCl) additional products are formed.<sup>6</sup> Structure B of Chart 1 and rotomeric isomers were proposed in order to account for all products within one coordination pattern although it was pointed out that the additional signals might arise from products of different coordination from the major products.<sup>6,7</sup> This work supports the latter interpretation.

At present, the structure of any of the minor products is not known, nor is there sufficient information available for reasonable speculation. It is, however, known that diols can give rise to major products that are chemically distinct from those characterized in this study. For instance, although both  $\alpha$ - and  $\beta$ -methyl galactosides give rise to 2:2 complexes with vanadium NMR signals at –521 ppm, an additional 2:2 product with a signal at –502 ppm is also formed.<sup>4</sup> This latter product can incorporate at least one additional ligand and therefore probably has octahedral coordination about the two vanadiums. A similar product has not been observed to form in the presence of nucleosides nor has it been found that the products investigated here can incorporate a third ligand, although a mixed bis-ligand product can be formed.<sup>8,24</sup>

**Acknowledgment.** A.S.T. acknowledges the occurrence of numerous discussions, agreements and disagreements, with William J. Ray, Jr., of Purdue University and Debbie C. Crans, at Colorado State University, concerning the structure of dimeric vanadium complexes formed with diols. In addition, thanks are gratefully extended to NSERC, Canada (A.S.T. and F.W.B.E.), for its financial support of this work.

**Supplementary Material Available:** FT infrared spectra for adenosine and product complex and listings of fractional atomic coordinates and temperature factors, intramolecular distances and angles, additional crystallographic details, hydrogen atom parameters, anisotropic thermal parameters, additional bond lengths and angles, torsion angles, and distances and angles associated with hydrogen bonds (23 pages). This material is contained in many libraries on microfiche, immediately follows this article in the microfilm version of the journal, can be ordered from the ACS, and can be downloaded from the Internet; see any current masthead page for ordering information and Internet access instructions.

JA943891H